doi.org/10.36721/PJPS.2026.39.12.334.1

# Artemisinin alleviates hippocampal neuronal apoptosis and cognitive impairment in rats after cardiac arrest resuscitation: Association with the PI3K/Akt pathway

**Yuanyuan Gao[1#], Shuwen Han[1#], Yaojun Lu[2*] and Junli Zhao[3*]**
[1]Affiliated Baotou Clinical College of Inner Mongolia Medical University, Baotou, Inner Mongolia, 014042, China
[2]Department of Cardiology, Baotou Central Hospital, Baotou, Inner Mongolia, 014042, China
[3]Department of Pharmacy, Baotou Central Hospital, Baotou, Inner Mongolia, 014042, China

**Abstract**: **Background**: Cardiac arrest (CA) is associated with high mortality and severe neurological sequelae. Artemisinin (ARS), a natural product from Artemisia annua, has potential neuroprotective effects, but its role in brain injury after CA resuscitation remains unclear. **Objectives**: This study investigated the effects of ARS on hippocampal neuronal apoptosis and cognitive dysfunction in rats after CA resuscitation and explored whether these effects are associated with the phosphatidylinositol 3-kinase/protein kinase B (PI3K/Akt) signaling pathway. **Methods**: Sixty male rats were randomly assigned to six groups: sham, model, artemisinin (40 mg/kg), dimethyl sulfoxide ((DMSO, 100 mg/kg), LY294002 (a phosphatidylinositol 3-kinase inhibitor, 25 mg/kg) and artemisinin plus LY294002. Cardiac arrest was induced by transcutaneous electrical stimulation. Outcome assessors were blinded. Neurological function was evaluated using the Neurological Deficit Scale. Hippocampal damage and apoptosis were assessed by hematoxylin and eosin staining and terminal deoxynucleotidyl transferase dUTP nick end labeling staining. Learning and memory were tested using novel object recognition and the Morris water maze. Protein expression was measured by Western blot. **Results**: Artemisinin significantly improved Neurological Deficit Scale scores, reduced terminal deoxynucleotidyl transferase dUTP nick end labeling-positive cells and alleviated hippocampal damage. Artemisinin also prolonged novel object exploration time, shortened escape latency, increased target quadrant time and upregulated phosphatidylinositol 3-kinase expression and the ratio of phosphorylated protein kinase B to protein kinase B. Co-administration of LY294002 partially reversed these effects. **Conclusion**: Artemisinin alleviates hippocampal neuronal apoptosis and improves neurological deficits and cognitive dysfunction in rats after cardiac arrest resuscitation, suggesting a possible association with activation of the phosphatidylinositol 3-kinase/protein kinase B pathway. Limitations include use of a single pharmacological inhibitor and lack of genetic validation.

**Keywords**: Artemisinin; PI3K/Akt; Cardiac arrest; Cognitive function; Neuronal apoptosis

*Submitted on 27-03-2026 – Revised on 13-05-2026 – Accepted on 15-06-2026*

## INTRODUCTION

Cardiac arrest (CA) is a pathological process caused by the sudden interruption of mechanical cardiac contraction and respiratory function, leading to cessation of systemic blood perfusion and tissue oxygenation, ultimately resulting in coma (Sayed *et al*., 2024). Epidemiological data indicate that the overall prognosis of patients with CA remains poor. Although approximately 30% of the patients can regain spontaneous circulation, the final discharge survival rate is less than 10% (Tseng and Nakasuka, 2025; Patterson *et al*., 2026). Therefore, identifying effective intervention targets for brain injury after CA resuscitation is crucial for improving patients' quality of life.

Brain injury after resuscitation results from oxidative stress, inflammation and apoptosis induced by cerebral ischemia-hypoxia and reperfusion (Kaito *et al*., 2025; Yuan *et al*., 2023). The hippocampus CA1 region is highly sensitive to cerebral ischemia-hypoxia and its neurons are prone to apoptosis after resuscitation, leading to impaired learning, memory and cognitive function (Beheshti *et al*., 2026). Neuronal apoptosis is regulated by multiple signaling pathways, among which the phosphatidylinositol 3-kinase (PI3K)/protein kinase B (Akt) pathway is a key regulator of the balance between cell survival and apoptosis (Cui *et al*., 2023). Previous studies have shown that enhancing PI3K/Akt pathway activity to inhibit excessive neuronal apoptosis is an important mechanism for alleviating brain injury after cardiac arrest resuscitation. Results from a porcine cardiac arrest model demonstrated that mild hypothermia alleviated cerebral ischemia-reperfusion injury by modulating the PI3K/Akt/mammalian target of rapamycin (mTOR) pathway and reducing complement C5a-induced neuronal autophagy and apoptosis (Wang *et al*., 2023). Artemisinin (ARS) is a sesquiterpene lactone active component in the Chinese herb Artemisia annua (Feng *et al*., 2025). In recent years, the biological effects of ARS in neuroprotection have attracted attention. A study on progressive neurodegenerative diseases (Mustafa *et al*., 2026) demonstrated that ARS intervention significantly reduced oxidative stress, inhibited programmed necrosis and upregulated neuroprotective markers, thereby

**Corresponding author:* e-mail: Luyaojun995@126.com; 18604729668@163.com
#These authors contributed equally and are the co-first authors.

exerting a powerful neuroprotective effect. Previous research has demonstrated that total phenolics from Hemerocallis citrina Baroni leaves exert neuroprotective effects in a corticosterone-induced PC12 neuronal cell damage model by activating the PI3K/AKT signaling pathway (Jia *et al*., 2024). However, whether ARS alleviates hippocampal neuronal apoptosis and improves cognitive dysfunction after CA recovery by regulating the PI3K/Akt signaling pathway remains unexplored. It was hypothesized that ARS activates the PI3K/Akt signaling pathway, thereby inhibiting hippocampal neuronal apoptosis and reducing neurological deficits and cognitive dysfunction after CA recovery. Based on this hypothesis, this experiment aims to explore the role and mechanism of ARS in regulating the PI3K/Akt pathway to reduce hippocampal neuronal apoptosis and improve cognitive function after CA recovery, with the aim of providing new directions for clinical practice.

## MATERIALS AND METHODS

### *Materials*

#### *Experimental rats*

Sixty specific pathogen-free (SPF)-grade male Sprague-Dawley (SD) rats (Chengdu Dashuo Experimental Animal LTD, Production License: SCXK (Shanghai) 2018-0003), aged 7-9 weeks and weighing 200-250 g, were selected. All rats were housed in a constant temperature and humidity environment (temperature 22 ± 2ºC, humidity 50 ± 10%). Each day, they were exposed to 12 hours of light and 12 hours of darkness, with free access to food and water. The rats were acclimated for 1 week before the experiment.

#### *Experimental reagents and equipment*

The experimental reagents and equipment are detailed in Tables 1 and 2.

### *Methods*

#### *Construction and grouping of rats for CA resuscitation*

Using the random number table method, 60 male SPF-grade SD rats were randomly divided into a sham operation group (n=10) and a model induction group (n=50). The 50 rats in the model induction group were subsequently randomly assigned to five subgroups (n=10 per subgroup): model group, ARS group, dimethyl sulfoxide (DMSO) group, LY294002 group and ARS+LY294002 group. The CA model was established by percutaneous electrical stimulation of the epicardium following the method described in reference (Wu *et al*., 2022). For anesthesia and intubation, the rats were fasted for 12 hours before the operation and were allowed to drink freely. Anesthesia was induced by intraperitoneal injection of pentobarbital sodium (50 mg/kg). After anesthesia, the femoral artery and femoral vein were cannulated for real-time blood pressure monitoring and drug administration. Following tracheal intubation, a small animal ventilator was connected for mechanical ventilation and the electrocardiogram (ECG) was recorded. Percutaneous electrical stimulation of the epicardium was performed with the parameters of frequency 50 Hz, current 5 mA and duration 3 minutes. The criterion for successful model construction was defined as: 10 seconds after the electrical stimulation, arterial pressure <25 mmHg with an approximately flat arterial pressure waveform, or ventricular fibrillation/ asystolic electrical activity on the ECG. If spontaneous heart rate recovery with mean arterial pressure >25 mmHg occurred within 3 minutes after electrical stimulation, the rat was excluded. For the resuscitation procedure, immediately after successful modeling, standard cardiopulmonary resuscitation (chest compression rate of 200 times/minute, ventilation rate of 60 times/minute) was performed. Successful return of spontaneous circulation (ROSC) was defined as restoration of sinus rhythm, arterial pressure >60 mmHg and stability for more than 10 minutes. Rats in the sham-operated group were subjected to the same surgical procedure as the model group, but without electrical stimulation and cardiopulmonary resuscitation.

#### *Drug administration plan and grouping*

*Drug preparation*: For LY294002 (PI3K inhibitor), 5 mg of LY294002 was dissolved in 325 μL of DMSO to prepare a 50 mmol/L stock solution, which was stored at low temperature. Before use, the stock solution was diluted with phosphate-buffered saline (PBS) to 100 μmol/L and allowed to return to room temperature prior to administration. For the artemisinin (ARS) solution, 40 mg of ARS was precisely weighed, dissolved in 0.2 mL of DMSO and normal saline was added to a total volume of 10 mL to obtain a working solution containing 2% DMSO at a concentration of 4 mg/mL. The solution was ultrasonicated for 10 minutes to aid dissolution. For the DMSO solvent control group, an equivalent volume of 2% DMSO in normal saline (without ARS) was prepared to match the DMSO concentration and injection volume of the ARS group.

*Grouping and administration*: Administration was initiated 10 minutes after return of spontaneous circulation and was performed once daily for 7 consecutive days. All drugs or vehicles were administered via intraperitoneal injection with a standard injection volume of 10 mL/kg body weight. The six groups were as follows: Sham group: Normal saline (10 mL/kg) was injected intraperitoneally; Model group: the same volume of normal saline (10 mL/kg) was injected intraperitoneally; ARS group: ARS solution (40 mg/kg ARS in 2% DMSO, 10 mL/kg) was injected intraperitoneally; DMSO group: DMSO (100 mg/kg) was injected intraperitoneally as a solvent control; LY294002 group: LY294002 (25 mg/kg in 0.5% DMSO, 10 mL/kg) was injected intraperitoneally; ARS+LY294002 group: ARS (40 mg/kg) and LY294002 (1.8 mg/kg) in 2% DMSO (10 mL/kg) were injected intraperitoneally.

**Table 1**: Main reagents.

| Name | Companies |
|---|---|
| DMSO | Beijing Solarbio |
| Hematoxylin-eosin staining kit | Beijing Solarbio |
| PCR premix | Beijing Nobel Biocare |
| PI3K primary antibody | Abcam (USA) |
| Akt primary antibody | Abcam (USA) |
| p-Akt primary antibody | Abcam (USA) |
| β-actin primary antibody | Abcam (USA) |
| Rabbit anti-mouse secondary antibody | Abcam (USA) |
| Artemisinin | Shanghai Aladdin Biotechnology |
| LY294002 | SIGMA L9908 (USA) |
| Tunel staining | Shenzhen Top |

**Table 2**: Main equipment.

| Equipment | Model | Manufacturer |
|---|---|---|
| Small animal ventilator | ALC-V8S | Shanghai Alcott Biotech Co., Ltd., Shanghai, China |
| High-speed refrigerated centrifuge | TGL-20M | Shandong Kebo Scientific Instruments Co., Ltd., Shandong, China |
| Refrigerated centrifuge | 5418 R | Eppendorf AG, Hamburg, Germany |
| Multichannel physiological recording system | PowerLab 16/35 | ADInstruments, Sydney, Australia |
| Electrical stimulator | Model S88 | Grass Technologies, West Warwick, RI, USA |
| Inverted fluorescence microscope | — | Nikon Corporation, Tokyo, Japan |
| Automated video tracking system | EthoVision XT 14 | Noldus Information Technology, Wageningen, the Netherlands |
| Gel electrophoresis system | Mini-protean tetra cell | Bio-Rad Laboratories, Hercules, CA, USA |
| Wet transfer system | — | Bio-Rad Laboratories, Hercules, CA, USA |
| Chemiluminescence imaging analysis system | ChemiDoc MP | Bio-Rad Laboratories, Hercules, CA, USA |
| Transmission electron microscope | — | Beijing Serki Technology Co., Ltd., Beijing, China |
| Rotary microtome | RM2255 | Leica Biosystems, Nussloch, Germany |
| Morris water maze apparatus | Custom-made | Zhongshi Digitals, Beijing, China |

Notably, the DMSO control group received an intraperitoneal injection of 100 mg/kg DMSO to match the DMSO content in the ARS solution (the ARS solution contained approximately 100 mg/kg DMSO based on the 4 mg/mL ARS in 2% DMSO solution, with a standard injection volume of 10 mL/kg body weight). This ensured that DMSO exposure was comparable between the DMSO control group and the ARS treatment group.

*Dose selection basis*: The ARS dose (40 mg/kg) was selected based on previous studies (Wang *et al*., 2024), in which this dose demonstrated significant neuroprotective effects in the rat model and no obvious toxicity was observed. The LY294002 dose (25 mg/kg) was selected based on the dosage used in previous studies (Ni *et al*., 2022).

*Rationale for DMSO control design*: To isolate the potential neuroprotective effects of DMSO from those of ARS, the DMSO control group administered 2% DMSO in normal saline at the same injection volume (10 mL/kg) as the ARS group. This design ensured that the DMSO concentration and volume were identical in the DMSO and ARS groups. However, it should be noted that this design did not fully control for potential interactions between DMSO and ARS, nor did it account for any pharmacological effects that may have arisen specifically from co-administration. This limitation is addressed in the Discussion section.

***Blinding design and assignment concealment***

*Blinding was implemented during outcome assessment*: behavioral tests, histopathological analyses and Western blot analyses were independently conducted by researchers unaware of group assignments.

***Sample size and power analysis***

Each group was designed to include 10 rats. Considering the mortality rate during CA model establishment and recovery (expected survival rate of approximately 50%), 50 rats were initially allocated to the model induction groups and 10 to the sham operation group, for a total of 60 rats. After the 7-day observation period, the final numbers of surviving rats in each group were as follows:

sham group, n=10; model group, n=5; ARS group, n=7; DMSO group, n=7; LY294002 group, n=4; ARS+LY294002 group, n=4. All behavioral, histological and Western blot analyses were conducted on these surviving animals. Power analysis indicated that, with an effect size of Cohen's d = 1.5 and alpha = 0.05, 5 rats per group would achieve statistical power exceeding 80% (Lange *et al*., 2026).

***Animal husbandry and environmental conditions***

All rats were housed in SPF-level animal rooms. The temperature was maintained at 22 ± 2 ℃, the humidity at 50% ± 10%, with a 12-hour light/12-hour dark cycle. The rats had free access to standard feed and water. During the experiment, the animals' conditions were observed daily and any abnormalities or deaths were recorded.

***Main observation indicators***

***Survival status of rats after surgery***

The survival rates of the rats in each group were statistically analyzed 24 hours after the restoration of spontaneous circulation (ROSC). The criteria for survival determination were the presence of spontaneous breathing, heart rate and mobility.

***Neurological deficit score***

Within 72 hours after the model was successfully established, neurological function was evaluated using the Neurological Deficit Scale (NDS) (Geocadin *et al*., 2000). This scale covered five aspects: behavior, sensation, motor function, autonomous activities and epileptic seizures, with a total score ranging from 0 to 100. A higher score indicated better recovery of neurological function. The scores were independently completed by two researchers who were blinded to group assignments and the mean was calculated.

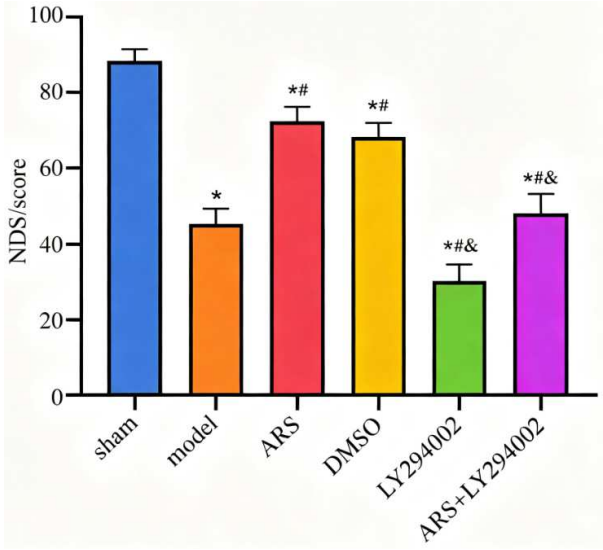


**Fig. 1**: Comparison of NDS scores among rat groups. (Note: *P<0.05 compared with the Sham group; #P<0.05 compared with the Model group; &P<0.05 compared with the ARS group. NDS: Neurological deficit scale)

***Histopathological observation of hippocampal tissue in rats with hematoxylin and eosin (HE) staining***

The rats were sacrificed 72 hours after ROSC. Their heads were decapitated to obtain the brains and the hippocampal tissues were separated (refer to Step 2.3.7). The tissues were fixed with 4% paraformaldehyde. After gradient ethanol dehydration and xylene clearing, they were embedded in paraffin, sectioned at 4 μm, stained with HE and mounted. The neuronal morphology in the CA1 region was observed under a light microscope.

***Terminal deoxynucleotidyl transferase dUTP nick end labeling (TUNEL) detection of neuronal apoptosis***

For each group, 3 rats were randomly selected and their brains were taken, embedded in paraffin and sectioned (4 μm). After dewaxing and hydration, antigen retrieval was performed using proteinase K and the TUNEL reaction solution was incubated at 45°C in the dark for 2 hours. The cell nuclei were re-stained with 4',6-diamidino-2-phenylindole (DAPI) for 10 minutes. Under a fluorescence microscope (green channel: Ex/Em = 488 nm/525 nm; blue channel: Ex/Em = 358 nm/461 nm), 5 fields of view were randomly selected from each section and the apoptosis rate was calculated. This was carried out according to the previously reported method (Guo *et al*., 2024).

***Rat learning and memory ability testing***

*Morris water maze experiment*: The water tank had a diameter of 150 cm, a height of 50 cm and a water depth of 25 cm. The experiment was divided into the navigation positioning experiment (5 days, 4 training sessions per day, during which the escape latency was recorded) and the spatial exploration experiment (on the 6th day, the platform was removed and the time spent in the target quadrant and the number of platform crossings were recorded) (Cheng *et al*., 2024).

*New object recognition (NORT) experiment*: The experiment was divided into the adaptation period (3 days), the training period (10 minutes) and the test period (10 minutes), during which the exploration time for new and old objects was recorded by an automatic tracking system.

***Detection of PI3K, Akt and p-Akt proteins in hippocampal tissue (Western blot)***

Hippocampal tissue was extracted, ground in liquid nitrogen and lysed with radioimmunoprecipitation assay (RIPA) buffer. Total protein concentration was determined using the bicinchoninic acid (BCA) method. Proteins were separated by sodium dodecyl sulfate-polyacrylamide gel electrophoresis (SDS-PAGE) and transferred to a membrane. The membrane was blocked with 5% skimmed milk and incubated with primary antibodies (PI3K, Akt, p-Akt, β-actin, Abcam, 1:1000) at 4ºC overnight, followed by incubation with the secondary antibody at room temperature for 1 hour. Enhanced chemiluminescence (ECL) detection was performed and

the gray values were analyzed using ImageJ software. This was carried out according to the method described in the reference (Melo *et al*., 2026).

***Identification and separation of hippocampal tissue***

After the rats were decapitated and their brains were removed, the brain was divided into left and right hemispheres along the longitudinal fissure. Under a stereomicroscope, a curved, bulging structure corresponding to hippocampal tissue could be observed on the inner surface of the brain hemisphere. Using a micromanipulator, the hippocampal tissue was carefully dissected from the head end to the tail end of the hippocampus (as shown in Fig. 2A, where the hippocampal CA1 region is indicated by a bright yellow arc-shaped strip). The separated hippocampal tissue was immediately fixed or frozen for storage.

***Statistical analysis***

Data were processed using SPSS 27.0 software. All measurement data were expressed as mean ± standard error. Comparisons among multiple groups were conducted using one-way analysis of variance (ANOVA). Where the results of the ANOVA indicated statistically significant differences among the groups, Tukey's post hoc test was further employed for pairwise comparisons to control the type I error rate of multiple comparisons. The chi-square test or Fisher's exact test was used for comparisons between two groups. $P < 0.05$ was considered statistically significant. All behavioral, histological and Western blot data analyses were conducted in actual living animals (n = 5 - 10 per group).

## RESULTS

***Comparison of survival rates and neurological function impairment scores among different groups of rats***

At 24 hours after return of spontaneous circulation, survival numbers and rates in each group were as follows: sham group, 10/10 (100%); model group, 5/10 (50%); artemisinin group, 7/10 (70%); DMSO group, 7/10 (70%); LY294002 group, 4/10 (40%); artemisinin plus LY294002 group, 4/10 (40%). The survival rate of the model group was significantly lower than that of the sham group (P = 0.033, Fisher's exact test). The survival rate of the artemisinin group was not significantly different from that of the model group (P = 0.673, chi-square test). The survival rates of the LY294002 group and the artemisinin plus LY294002 group were significantly lower than that of the model group (P = 0.045 for both comparisons, Fisher's exact test).

Compared with the sham operation group (88.20 ± 3.10 points), the NDS score of the model group (45.60 ± 4.20 points) was significantly lower ($P < 0.001$, 95% CI: 33.54 to 51.72, Cohen's d = 4.121). Compared with the model group, the NDS score of the ARS group (72.40 ± 3.80 points) was significantly higher (P=0.000, 95% CI: 17.83 to 35.82, Cohen's d = 3.012), while the NDS score of the LY294002 group (30.10 ± 4.50 points) was further decreased (P = 0.042, 95% CI: 4.23 to 26.82, Cohen's d = 1.985). Compared with the ARS group, the NDS score of the ARS+LY294002 group (48.30 ± 5.00 points) was significantly lower ($P < 0.001$, 95% CI: 13.52 to 34.71, Cohen's d = 2.543). For comparisons between the model and sham groups and between the ARS and model groups, all $P < 0.001$; the comparison between the LY294002 and model groups yielded P = 0.042 (Fig. 1).

***Comparison of pathological histological changes of neurons in the CA1 region of the hippocampus in each group of rats***

The HE staining results are shown in Fig. 2. In the sham group, neurons in the hippocampal CA1 region were arranged closely and orderly, with clear layers, intact cell morphology and prominent nucleoli. In the model group and the DMSO group, loose and disordered cell arrangement, cell edema, nuclear shrinkage and hyperchromatism and vacuolar degeneration in the cytoplasm were observed. In the artemisinin group, the number of hyperchromatic neurons was reduced and cell arrangement was more regular compared with the model group. In the LY294002 group, neuronal loss and necrosis were observed. Compared with the artemisinin group, the artemisinin plus LY294002 group showed an increased number of hyperchromatic neurons and more severe disarray in cell arrangement.

***Comparison of the apoptosis rate of neurons in the CA1 region of the hippocampus in each group of rats***

Terminal deoxynucleotidyl transferase dUTP nick end labeling staining results are shown in figures. 3A and 3B. One-way analysis of variance revealed a significant difference in the number of terminal deoxynucleotidyl transferase dUTP nick end labeling-positive cells among the groups [$F(5, 29) = 15.412$, $P = 4.3 \times 10^{-8}$, $\eta^2 = 0.732$]. Compared with the sham group (2.31 ± 0.51 cells/field), the model group showed a higher number of terminal deoxynucleotidyl transferase dUTP nick end labeling-positive cells (28.60 ± 3.20 cells/field; $P = 4.3 \times 10^{-8}$, 95% confidence interval: 18.52 to 34.14, Cohen's d = 6.123). Compared with the model group, the artemisinin group showed a lower number of terminal deoxynucleotidyl transferase dUTP nick end labeling-positive cells (12.41 ± 2.11 cells/field; $P = 4.3 \times 10^{-8}$, 95% confidence interval: 8.33 to 24.14, Cohen's d = 3.454), while the LY294002 group showed a higher number (35.21 ± 4.03 cells/field; P = 0.038). Compared with the artemisinin group, the artemisinin plus LY294002 group showed a higher number of terminal deoxynucleotidyl transferase dUTP nick end labeling-positive cells (22.8 ± 3.52 cells/field; P = 0.002, 95% confidence interval: 4.53 to 16.32, Cohen's d = 2.011).

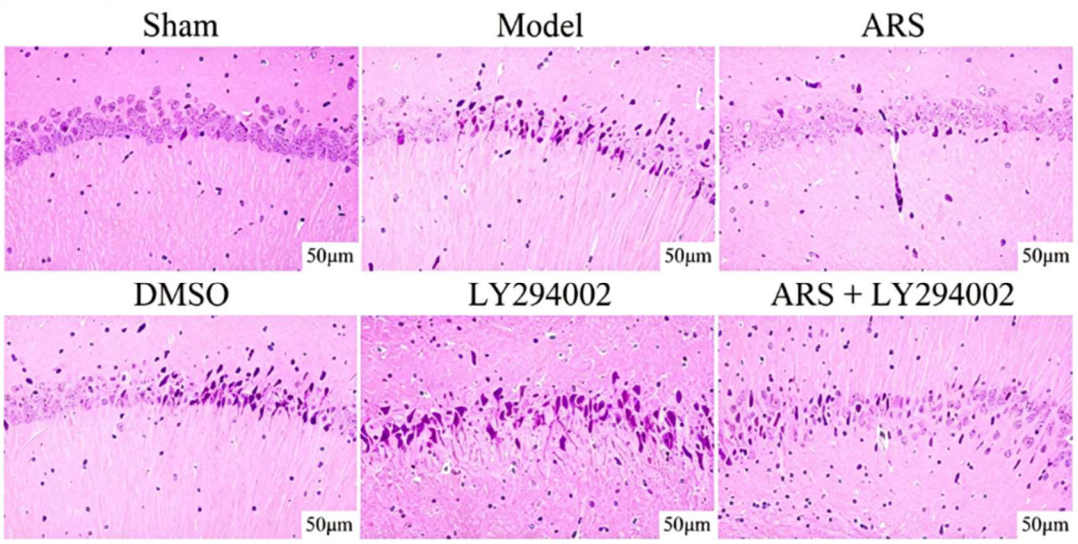


**Fig. 2**: H and E staining pathological image. 400×, scale bar, 50 μm.

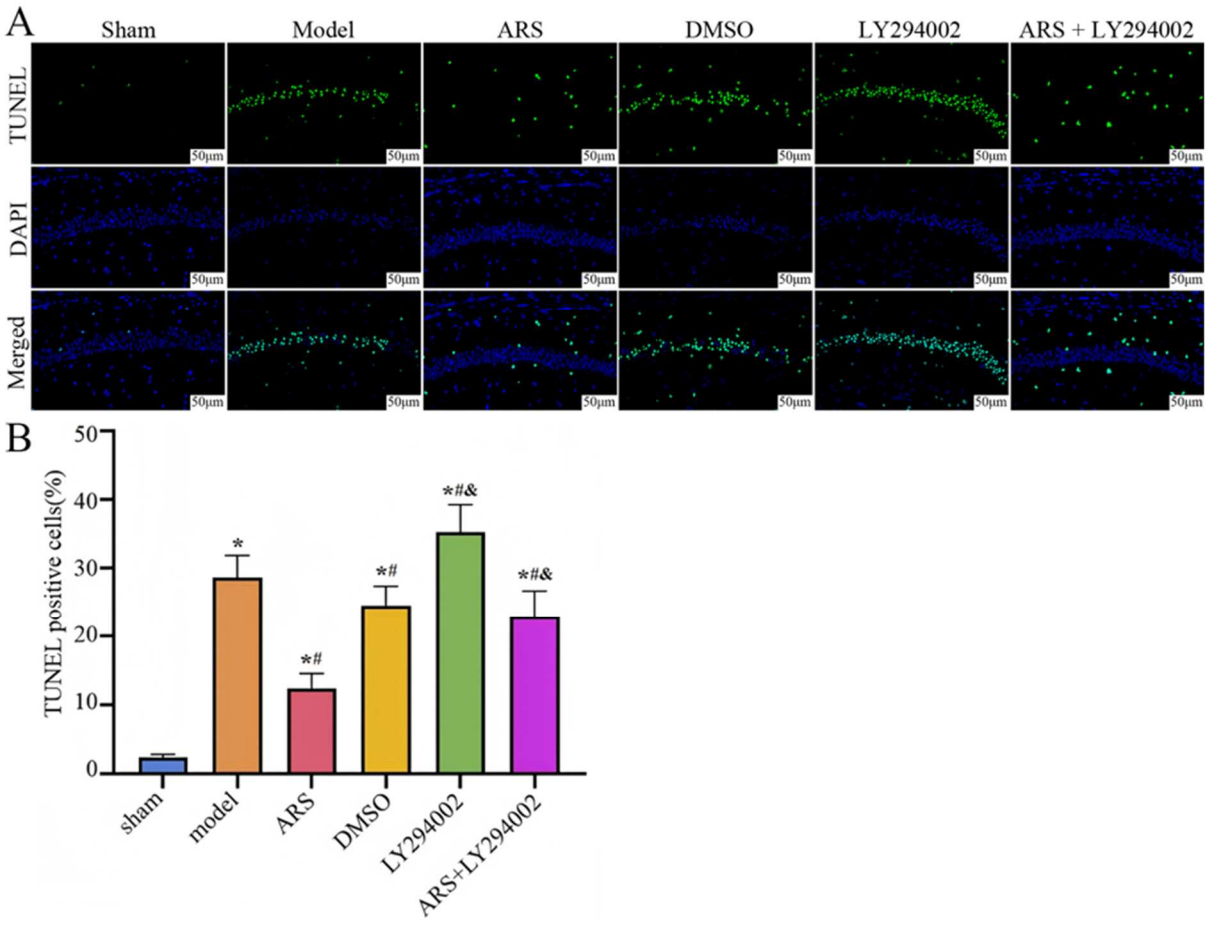


**Fig. 3**: TUNEL staining and quantification of apoptotic cells.
(A) TUNEL staining to assess hippocampal neuronal apoptosis in rats after CA resuscitation, scale bar: 50 μm; (B) Quantification of TUNEL+ cells, n=10. *P<0.05 compared to the Sham group; #P<0.05 compared to the Model group; &P<0.05 compared to the ARS group.

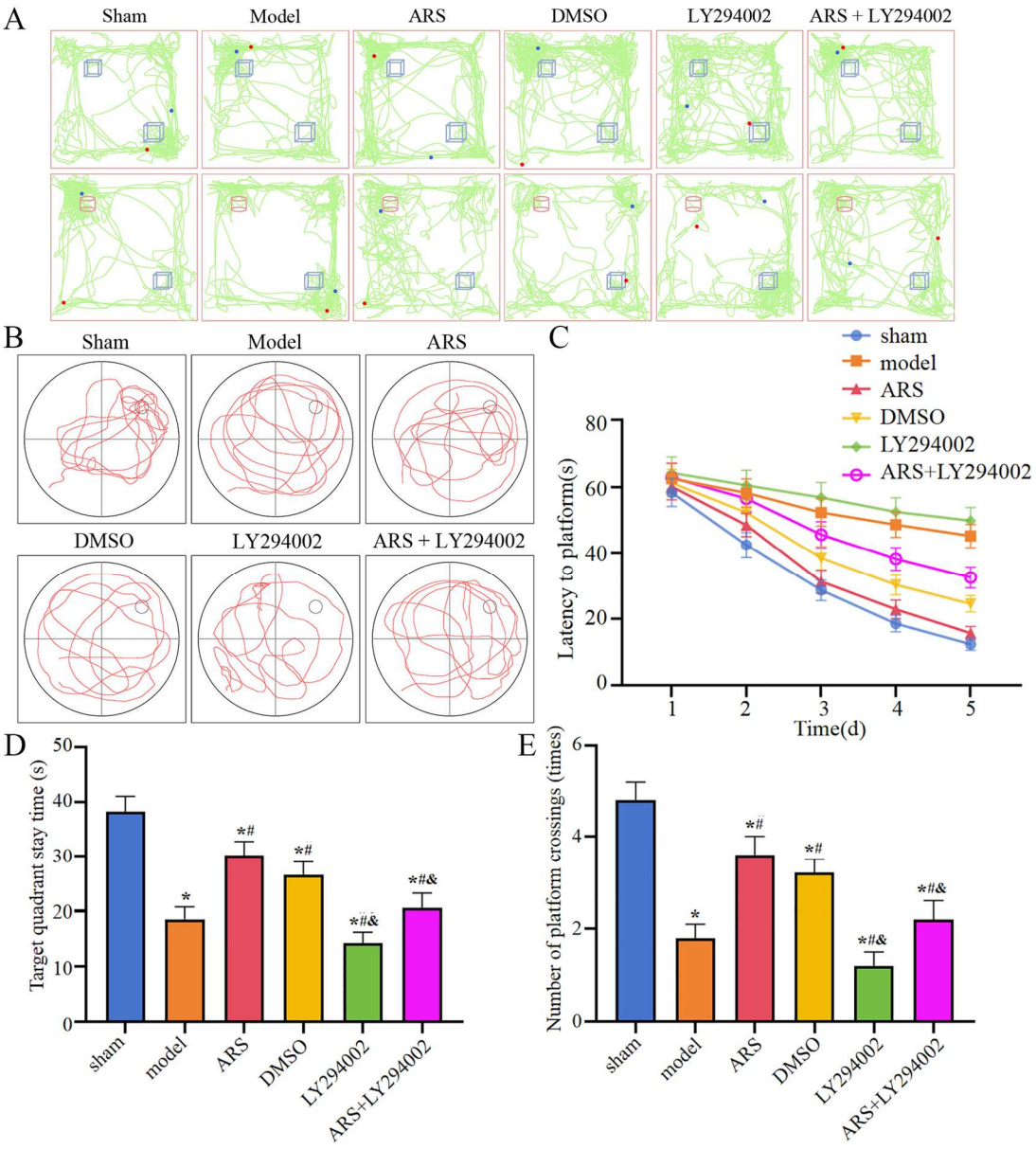


**Fig. 4**: ARS improves the learning and memory abilities of rats after CA resuscitation.
(A) Representative traces from each group in the NORT test; (B) Swimming traces from each group in the probe test; (C) Escapement latency line graph; (D) Target quadrant staying time bar chart; (E) Bar chart of the number of platform crossings. *P<0.05 compared to the Sham group; #P<0.05 compared to the Model group; &P<0.05 compared to the ARS group.

***Comparison of learning and memory abilities among different groups of rats***

***Results of the NORT experiment***

Novel object recognition test results are shown in fig. 4A. One-way analysis of variance revealed a significant difference in novel object exploration time among the groups [$F(5, 29) = 11.281$, $P = 2.6 \times 10^{-8}$, $\eta^2 = 0.662$]. Compared with the sham group (42.50 ± 3.11 seconds), the model group showed shorter novel object exploration time (18.61 ± 2.52 seconds; $P = 2.6 \times 10^{-8}$, 95% confidence interval: 15.21 to 32.62, Cohen's d = 5.011). Compared with the model group, the artemisinin group showed longer novel object exploration time (34.21 ± 2.82 seconds; $P = 2.6 \times 10^{-8}$, 95% confidence interval: 8.52 to 22.73, Cohen's d = 3.221), while the LY294002 group showed shorter exploration time (12.80 ± 2.21 seconds; P = 0.041, 95% confidence interval: 1.01 to 10.62, Cohen's d = 1.323). Compared with the artemisinin group, the artemisinin plus LY294002 group showed shorter novel object exploration time (21.51 ± 3.02 seconds; $P = 2.6 \times 10^{-8}$, 95% confidence interval: 5.62 to 19.83, Cohen's d = 2.451). The swimming traces of each group during the probe test are shown in figure 4B.

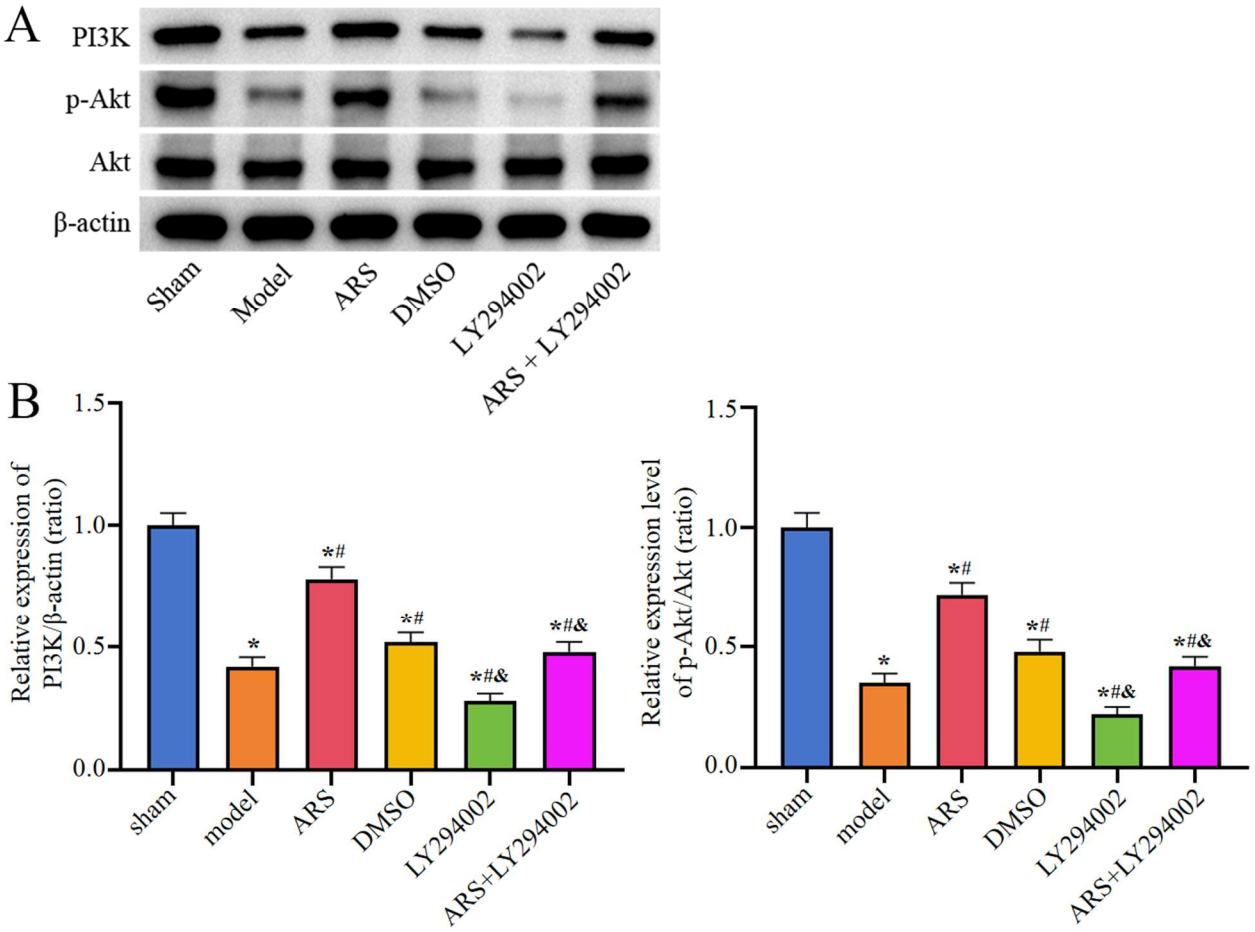


**Fig. 5**: ARS upregulates PI3K/Akt pathway protein expression in the hippocampus of rats after CA resuscitation. (A) Western blotting to determine PI3K, Akt, and p-Akt protein expression; (B) Density analysis of PI3K and p-Akt protein levels, with β-actin as a protein load control, n=10. *P<0.05 compared to the Sham group; #P<0.05 compared to the Model group; &P<0.05 compared to the ARS group.

***Morris water maze experiment***

Morris water maze navigation test results are shown in figure 4C. On day 3 of training, a one-way analysis of variance revealed a significant difference in escape latency between the model and artemisinin groups. Compared with the model group (52.31 ± 4.12 seconds), the artemisinin group showed shorter escape latency (31.21 ± 3.35 seconds; P = 3.9 × $10^{-8}$, 95% confidence interval: 12.52 to 29.71, Cohen's d = 2.981). Spatial probe test results are shown in figures. 4D and 4E. One-way analysis of variance revealed a significant difference in target quadrant dwell time among the groups [F(5, 29) = 13.56, P = 6.8 × $10^{-8}$, $\eta^2$ = 0.701]. Compared with the sham group (38.21 ± 2.82 seconds), the model group showed shorter target quadrant dwell time (18.51 ± 2.21 seconds; P = 6.8 × $10^{-8}$, 95% confidence interval: 12.41 to 27.02, Cohen's d = 4.211). Compared with the model group, the artemisinin group showed longer target quadrant dwell time (30.10 ± 2.50 seconds; P = 6.8 × $10^{-8}$, 95% confidence interval: 5.81 to 17.42, Cohen's d = 2.891), while the LY294002 group showed shorter dwell time (14.20 ± 2.01 seconds; P = 0.045, 95% confidence interval: 0.8 to 7.8, Cohen's d = 1.181). Compared with the artemisinin group, the artemisinin plus LY294002 group showed shorter target quadrant dwell time (20.51 ± 2.72 seconds; P = 0.002, 95% confidence interval: 3.2 to 16.0, Cohen's d = 2.04). One-way analysis of variance revealed a significant difference in the number of platform crossings among the groups [F(5, 29) = 12.04, P = 1.4 × $10^{-8}$, $\eta^2$ = 0.673]. Compared with the sham group (4.80 ± 0.40 times), the model group showed fewer platform crossings (1.80 ± 0.30 times; P = 1.4 × $10^{-8}$, 95% confidence interval: 1.82 to 4.23, Cohen's d = 4.561). Compared with the model group, the artemisinin group showed more platform crossings (3.60 ± 0.40 times; P = 1.4 × $10^{-8}$, 95% confidence interval: 1.01 to 2.62, Cohen's d = 2.781), while the LY294002 group showed fewer platform crossings (1.20 ± 0.30 times; P = 0.039, 95% confidence interval: 0.11 to 1.12, Cohen's d = 0.980). Compared with the artemisinin group, the artemisinin plus LY294002 group showed fewer platform crossings (2.20 ± 0.40 times; P = 0.003, 95% confidence interval: 0.51 to 2.32, Cohen's d = 2.101).

***Comparison of the protein expression levels of PI3K, Akt and p-Akt in the hippocampal tissues of each group of rats***

Western blot results are shown in figures. 5A and 5B. One-way analysis of variance revealed a significant difference in phosphatidylinositol 3-kinase protein expression among the groups [$F(5, 29) = 10.85$, $P = 2.5 \times 10^{-8}$, $\eta^2 = 0.650$]. Compared with the sham group (normalized to 1.00 ± 0.05), the model group showed lower phosphatidylinositol 3-kinase expression (0.42 ± 0.04; $P = 2.5 \times 10^{-8}$, 95% confidence interval: 0.38 to 0.78, Cohen's d = 5.120). Compared with the model group, the artemisinin group showed higher phosphatidylinositol 3-kinase expression (0.78 ± 0.05; $P = 2.5 \times 10^{-8}$, 95% confidence interval: 0.21 to 0.51, Cohen's d = 3.450), while the LY294002 group showed lower expression (0.28 ± 0.03; P = 0.032). Compared with the artemisinin group, the artemisinin plus LY294002 group showed lower phosphatidylinositol 3-kinase expression (0.48 ± 0.04; $P = 2.5 \times 10^{-8}$, 95% confidence interval: 0.15 to 0.45, Cohen's d = 2.980).

One-way analysis of variance revealed a significant difference in the ratio of phosphorylated protein kinase B to protein kinase B among the groups [$F(5, 29) = 14.221$, $P = 8.2 \times 10^{-8}$, $\eta^2 = 0.711$]. Compared with the sham group (1.00 ± 0.06), the model group showed a lower ratio (0.35 ± 0.04; $P = 8.2 \times 10^{-8}$, 95% confidence interval: 0.42 to 0.88, Cohen's d = 5.562). Compared with the model group, the artemisinin group showed a higher ratio (0.72 ± 0.05; $P = 8.2 \times 10^{-8}$, 95% confidence interval: 0.22 to 0.52, Cohen's d = 3.89), while the LY294002 group showed a lower ratio (0.22 ± 0.03; P = 0.028, 95% confidence interval: 0.03 to 0.23, Cohen's d = 1.321). Compared with the artemisinin group, the artemisinin plus LY294002 group showed a lower ratio (0.42 ± 0.04; $P = 8.2 \times 10^{-8}$, 95% confidence interval: 0.15 to 0.45, Cohen's d = 2.871). No significant difference in total protein kinase B protein expression was detected among the groups ($F(5, 29) = 0.421$, P = 0.832).

## DISCUSSION

According to epidemiological survey data (Andrea *et al*., 2024; Cagino *et al*., 2023), more than 200,000 in-hospital CA cases are recorded annually in the United States, of which approximately 40%–70% of patients achieve ROSC; however, the survival rate of patients after ROSC improves slowly, with a final survival rate of only 25%, which adversely affects patients' quality of life. ARS is the core active ingredient of the traditional Chinese medicine Artemisia annua. Studies have shown (Li *et al*., 2025) that ARS intervention in the CA rat model can increase the survival rate after resuscitation from 33.33% to 83.33%, which has good application value. In this experiment, a CA resuscitation rat model was established and ARS was used to intervene in the CA resuscitation rats to observe its effect on improving hippocampal neurons and cognitive function in CA resuscitation rats, as well as its effect on PI3K and Akt levels.

This study found that ARS treatment could increase the 24-hour survival rate of rats after CA resuscitation from 50% to 70% and the NDS score from 45.6 points to 72.4 points. This result is consistent with a previous study (Li *et al*., 2025) conducted in a CA rat model, which showed that the artemisinin derivative could increase the post-resuscitation survival rate from 33.33% to 83.33%. Moreover, this study directly compared the effects of ARS and DMSO groups in the CA model for the first time and the results showed that there were differences in the NDS scores between the two groups, suggesting that ARS has an independent protective effect beyond the solvent. This protective effect may be attributable to the antioxidant and anti-inflammatory properties of ARS. Previous studies have shown that ARS can alleviate ischemia-reperfusion injury by eliminating oxygen-free radicals and inhibiting the release of inflammatory factors (Jiang *et al*., 2022; Peng *et al*., 2022).

The results of this study showed that the number of TUNEL-positive cells in the CA1 area of the hippocampus increased significantly after CA resuscitation, while ARS treatment reduced it to 12.4 cells per field. Correspondingly, the exploration time of the new object recognition experiment and the target quadrant stay time in the water maze experiment of the ARS treatment group were significantly better than those of the model group. This result is consistent with previous studies in brain ischemia/reperfusion models. It is worth noting that this study also conducted two behavioral tests, NORT and the water maze, to evaluate recognition memory and spatial memory, respectively. The results of the two experiments showed a highly consistent trend, indicating that ARS can effectively improve the cognitive dysfunction in rats after CA resuscitation. This provides multiple perspectives of behavioral evidence for the neuroprotective effect of ARS.

The core mechanism discovered in this study is as follows: After ARS treatment, the expression levels of PI3K and the p-Akt/Akt ratio in hippocampal tissue significantly increased, while the total Akt level showed no significant change. More importantly, the PI3K inhibitor LY294002 can partially reverse the protective effect of ARS: Under the intervention of LY294002, the PI3K/Akt activation induced by ARS was inhibited and the neuroprotective effect weakened. This result supports the hypothesis that ARS inhibits neuronal apoptosis by activating the PI3K/Akt pathway. Compared with other neuroprotective studies in CA/resuscitation models, the findings of this study are unique. Previous studies in the mouse CA resuscitation model (Wang *et al*., 2022) found that Manganese porphyrin could reduce the mortality rate of hippocampal neurons to 39.00%; another brain ischemia-reperfusion model also confirmed (Chunchai *et*

*al*., 2022) that the administration of erythropoietin through activating the PI3K/Akt pathway could alleviate hippocampal neuronal apoptosis. This study is the first to provide preliminary evidence of the regulatory effect of ARS on the PI3K/Akt pathway in the CA resuscitation rat model.

Furthermore, although the DMSO control group received the same concentration and volume of DMSO as the ARS group, it remains possible that co-administration of DMSO with ARS in the treatment group may produce distinct pharmacokinetic or pharmacodynamic interactions not captured by the DMSO-only control. Future studies should consider additional control groups, such as a group receiving a different solvent vehicle, to more fully isolate the specific effects of artemisinin. The results showed that the NDS score and the number of TUNEL-positive cells in the DMSO group were between those of the model and ARS groups, suggesting that DMSO may have some neuroprotective effects. This finding is consistent with previous studies demonstrating that DMSO exerts free-radical-scavenging and anti-inflammatory effects at high doses (Huang *et al*., 2022; Akiyama *et al*., 2024). However, the protective effect of the ARS group was significantly better than that of the DMSO group, indicating that the protective effect of ARS is not entirely attributed to the solvent.

Secondly, regarding the variability induced by the model: In the CA model of this study, the final survival rate of the model group was only 50% and the survival rates of the LY294002 and ARS+LY294002 groups were even lower. This higher mortality rate may introduce selection bias, as surviving animals may represent a "healthier" subgroup. However, all the anesthesia, intubation, electrical stimulation and resuscitation operations in this study were performed by the same experienced researchers and all operations followed standardized protocols to minimize operational variability. Regarding blood-brain barrier permeability and pharmacokinetics, ARS was administered by intraperitoneal injection in this study and its concentration in brain tissue or blood-brain barrier permeability was not directly detected. However, existing literature supports that ARS has good blood-brain barrier penetration ability (Taubenschmid-Stowers *et al*., 2023; Kiss *et al*., 2024). Although this study did not directly detect the concentration of ARS in brain tissue, the Western blot results and behavioral results indirectly support that ARS can penetrate the blood-brain barrier and exert central nervous system protective effects.

## CONCLUSION

In conclusion, the findings of this study suggest that artemisinin alleviates neuronal apoptosis in the CA1 region of the hippocampus, improves neurological deficits and ameliorates cognitive dysfunction in rats after CA resuscitation and its protective effect is related to the activation of the PI3K/Akt pathway. However, the experimental design of this study focused primarily on the PI3K/Akt pathway and did not directly assess oxidative stress or inflammatory markers. Therefore, the above mechanisms still need further verification. In addition, the potential confounding effect of DMSO as a solvent was not adequately controlled. In terms of mechanistic validation, this study used only LY294002 as a pharmacological inhibitor and the LY294002 group included only 4 animals. The statistical power was limited. At the same time, this study did not use genetic validation methods such as gene knockout or overexpression, nor did it detect changes in the activity of downstream molecules and apoptotic execution proteins in the pathway. Therefore, the depth of the mechanism verification remains limited. Moreover, this study did not analyze the pharmacokinetics of ARS and its efficiency in crossing the blood-brain barrier is still unclear.Future studies should combine pharmacokinetic analysis, genetic validation and more comprehensive molecular detection to further verify the results of this study.

***Acknowledgments***
The authors thank the laboratory staff at Affiliated Baotou Clinical College of Inner Mongolia Medical University for their technical assistance during animal experiments and sample processing. We also thank the Animal Experimental Center for providing animal care and housing facilities.

***Author's contributions***
Yuanyuan Gao: Methodology, investigation, data curation, validation and visualization; Shuwen Han: Methodology, investigation, resources and validation; Yaojun Lu: Conceptualization, supervision, project administration, funding acquisition, writing – review and editing; Junli Zhao: Designed the study, performed the experiments, analyzed and interpreted the data, drafted the manuscript and approved the final version for publication.

***Funding***
There was no funding.

***Data availability statement***
The datasets generated during and/or analysed during the current study are available from the corresponding author on reasonable request.

***Ethical approval***
This study was approved by the ethics committee of Affiliated Baotou Clinical College of Inner Mongolia Medical University (Approval Number: 2025-YJS-067). This study was performed in adherence with the ARRIVE guidelines. See supplementary file for the ARRIVE checklist.

***Conflict of interest***
The authors declare no conflict of interest.

***Supplementary data***
https://pjps.pk/uploads/2026/08/SUP1787570583.pdf

## REFERENCES


Akiyama Y, Niimi A, Nomiya A, Taguchi S, Yamada Y, Sato Y, Kawai T, Yamada D, Kume H and Homma Y (2024). Efficacy and safety of intravesical dimethyl sulfoxide treatment for patients with refractory Hunner-type interstitial cystitis: Real-world data postofficial approval in Japan. *Int J Urol*., **31**(2): 111-118.

Andrea L, Herman NS, Vine J, Berg KM, Choudhury S, Vaena M, Nogle JE, Halablab SM, Kaviyarasu A, Elmer J, Wardi G, Pearce AK, Crowley C, Long MT, Herbert JT, Shipley K, Bissell Turpin BD, Lanspa MJ, Green A, Ghamande SA and Society of Critical Care Medicine's Discovery, the Critical Care Research Network DISCOVER In-Hospital Cardiac Arrest (DISCOVER IHCA): Investigator Group (2024). The discover in-hospital cardiac arrest (discover ihca) study: an investigation of hospital practices after in-hospital cardiac arrest. *Crit Care Explor*., **6**(9): e1149.

Beheshti S, Badiyifard A, Badiei Darani Z, Azimzadeh M and Halabian A (2026). Pitolisant disrupts memory consolidation and hippocampal synaptic plasticity: Impaired excitability and long-term potentiation in the CA1 area. *Iran J Basic Med Sci*., **29**(3): 378-386.

Cagino LM, Moskowitz A, Nallamothu BK, McSparron J, Iwashyna TJ and American Heart Association's Get With The Guidelines-Resuscitation Investigators (2023). Trends in return of spontaneous circulation and survival to hospital discharge for in-intensive care unit cardiac arrests. *Ann Am Thorac Soc*., **20**(7): 1012-1019.

Cheng J, Wang Z, Yu H, Chen Y, Wang Z, Zhang L and Peng X (2024). The duration-dependent and sex-specific effects of neonatal sevoflurane exposure on cognitive function in rats. *Braz J Med Biol Res*., **57**: e13437.

Chunchai T, Apaijai N, Benjanuwattra J, Pintana H, Singhanat K, Arunsak B, Chattipakorn N and Chattipakorn SC (2022). Erythropoietin administration exerted neuroprotective effects against cardiac ischemia/reperfusion injury. *Curr Res Pharmacol Drug Discov*., **3**: 100124.

Cui Y, Yang B, Lin S, Huang L, Xie F, Feng W and Lin Z (2023). FGF23 alleviates neuronal apoptosis and inflammation and promotes locomotion recovery via activation of PI3K/AKT signalling in spinal cord injury. *Exp Ther Med*., **26**(1): 340.

Feng J, He Y, Bai T, You Q, Zhu H, Jia C, Liu B and Li S (2025). Bibliometric and visualized analysis of artemisinin and its derivatives in cancer. *Drug Des Devel Ther*., **19**: 5517-5538.

Geocadin RG, Ghodadra R, Kimura T, Lei H, Sherman DL, Hanley DF and Thakor NV (2000). A novel quantitative EEG injury measure of global cerebral ischemia. *Clin Neurophysiol*., **111**(10): 1779-1787.

Guo B, Qi M, Luo X, Guo L, Xu M, Zhang Y, Li Z, Li M, Wu R, Guan T, Liu M and Liu Y (2024). GIP attenuates neuronal oxidative stress by regulating glucose uptake in spinal cord injury of rat. *CNS Neurosci Ther*., **30**(6): e14806.

Huang Z, Peng R, Yu H, Chen Z, Wang S, Wang Z, Dong S, Li W, Jiang Q, Li F and Li Q (2022). Dimethyl sulfoxide attenuates radiation-induced testicular injury through facilitating DNA double-strand break repair. *Oxid Med Cell Longev*., **2022**: 9137812.

Jia Y, Wang Y, Wang Z, Zhang Z, Zhang J, Zhang J, Sun K, Hua Y, Chai G and Hu F (2024). Neuroprotective effects of total phenolics from Hemerocallis citrina Baroni leaves through the PI3K/AKT pathway. *Front Pharmacol*., **15**: 1370619.

Jiang M, Lai X, Zhang Y, Shen M, Ma H, Liu A, Wu J and Yan J (2022). Artemisinin alleviates cerebral ischemia/reperfusion-induced oxidative damage via regulating PHB2-mediated autophagy in the human neuroblastoma SH-SY5Y cell line. *Oxid Med Cell Longev*., **2022**: 6568748.

Kaito D, Tamura T, Suzuki S, Onishi R, Tanaka KF, Yoshino J, Matsuoka T, Maeshima K, Sasaki J and Homma K (2025). Systemic nicotinamide mononucleotide administration to mitigate post-cardiac arrest brain injury in mice. *PLoS One*., **20**(10): e0334608.

Kiss E, Kins S, Gorgas K, Venczel Szakács KH, Kirsch J and Kuhse J (2024). Another use for a proven drug: Experimental evidence for the potential of artemisinin and its derivatives to treat alzheimer's disease. *Int J Mol Sci*., **25**(8): 4165.

Lange KM, Sullivan TR, Kasza J and Yelland LN (2026). An online sample size calculator for designing partially clustered trials. *Clin Trials*., **23**(2): 225-231.

Li H, Cheng C, Liang L, Jin T, Zhang G, Peberdy MA, Ornato JP, Tang W and Yang M (2025). Artesunate preserves post-resuscitation myocardial and neurologic function in a rat model of cardiac arrest and cardiopulmonary resuscitation. *Resusc Plus*., **27**: 101214.

Melo MM, Phillippi ES, Schultz ML, Shen SQ and El-Shanti H (2026). Quantifying cytoskeletal protein interactions with far Western blotting. *Front Mol Biosci*., **13**: 1761723.

Mustafa AM, Mudhafar M, Elgindy AM, Esmail MM, Atwa AM, Shaheen AM, Radwan AF, Elfar N, Mohamed RYA and Gamil NM (2026). Artemisinin attenuates 3-nitropropionic acid-induced neurodegeneration via HMGB1/TLR4/NF-κB modulation in a rat model of huntington's disease. *Arch Pharm Res*., **49**(3): 375-392.

Ni RJ, Gao TH, Wang YY, Tian Y, Wei JX, Zhao LS, Ni

PY, Ma XH and Li T (2022). Chronic lithium treatment ameliorates ketamine-induced mania-like behavior via the PI3K-AKT signaling pathway. *Zool Res*., **43**(6): 989-1004.

Patterson T, Perkins GD, Dodd M, Perkins A, Mellett-Smith A, Fothergill RT, Clayton T, Evans R, Robertson S, Kwok M, Wilson K, McDonaugh B, McCrone P, Dalby M, Firoozi S, Malik I, Rakhit R, Jain A, MacCarthy P, Nolan JP and ARREST Trial Collaborators (2026). Expedited transfer to emergency department vs. cardiac catheter laboratory in a cardiac arrest centre for non-ST-elevation out-of-hospital cardiac arrest: ARREST trial as-treated analysis. *Eur Heart J Acute Cardiovasc Care*., **15**(1): 3-12.

Peng T, Li S, Liu L, Yang C, Farhan M, Chen L, Su Q and Zheng W (2022). Artemisinin attenuated ischemic stroke induced cell apoptosis through activation of ERK1/2/CREB/BCL-2 signaling pathway *in-vitro* and *in-vivo*. *Int J Biol Sci*., **18**(11): 4578-4594.

Sayed AI, Mobarki SJ, Hakami AA, Saabi SM, Oraibi MM, Darraj BH, Alshamakhi AH, Abuhadi HM, Abdulwali HM and Hakami AM (2024). Awareness, knowledge and attitudes regarding cardiopulmonary resuscitation in case of cardiac arrest among the population in the jazan region, Saudi Arabia. *Ann Afr Med*., **23**(2): 118-124.

Takenaka R, Matsumoto S, Nureki S, Wada S, Oyama Y, Sakamoto T, Kitano T and Shigemitsu O (2023). Real-time monitoring of vitamin C levels in trauma patients by electron-spin resonance spectrometry. *BMC Emerg Med*., **23**(1): 85.

Taubenschmid-Stowers J, Orthofer M, Laemmerer A, Krauditsch C, Rozsova M, Studer C, Lotsch D, Gojo J, Gabler L, Dyczynski M, Efferth T, Hagelkruys A, Widhalm G, Peyrl A, Spiegl-Kreinecker S, Hoepfner D, Bian S, Berger W, Knoblich JA, Elling U and Penninger JM (2023). A whole-genome scan for Artemisinin cytotoxicity reveals a novel therapy for human brain tumors. *EMBO Mol Med*., **15**(3): e16959.

Tseng ZH and Nakasuka K (2025). Out-of-hospital cardiac arrest in apparently healthy, Young adults. *JAMA*., **333**(11): 981-996.

Wang L, Sun Y, Kong F, Jiang Y, An M, Jin B, Cao D, Li R, Guan X, Liang S, Abudurexiti S and Gong P (2023). Mild hypothermia alleviates complement C5a-induced neuronal autophagy during brain ischemia-reperfusion injury after cardiac arrest. *Cell Mol Neurobiol*., **43**(5): 1957-1974.

Wang B, Zhu S, Guo M, Ma RD, Tang YL, Nie YX and Gu HF (2024). Artemisinin ameliorates cognitive decline by inhibiting hippocampal neuronal ferroptosis via Nrf2 activation in T2DM mice. *Mol Med*., **30**(1): 35.

Wang P, Li Y, Yan B, Yang Z, Li L, Cao Z, Li X, Batinic-Haberle I, Spasojevic I, Warner DS and Sheng H (2022). Manganese porphyrin promotes post cardiac arrest recovery in mice and rats. *Biology*., **11**(7): 957.

Wu SN, Tsai MS, Huang CH and Chen WJ (2022). Omecamtiv mecarbil treatment improves post-resuscitation cardiac function and neurological outcome in a rat model. *PLoS One*., **17**(2): e0264165.

Yuan Y, Tian Y, Jiang H, Cai LY, Song J, Peng R and Zhang XM (2023). Mechanism of PGC-1α-mediated mitochondrial biogenesis in cerebral ischemia-reperfusion injury. *Front Mol Neurosci*., **16**: 1224964.